AIAA JOURNAL
Vol. 35, No. 2, February 1997

Sensor Placement and Structural Damage Identification from Minimal Sensor Information

Richard G. Cobb* and Brad S. Liebst†
U.S. Air Force Institute of Technology, Wright–Patterson Air Force Base, Ohio 45433-7765

A method of prioritizing sensor locations on a flexible structure for the purpose of determining damaged structural elements from measured modal data is presented. This method is useful in applications where practicality dictates only a small subset of the total structural degrees of freedom can be instrumented. In such cases, it is desirable to place sensors in locations yielding the most information about the damaged structure. No a priori knowledge of the damage location is assumed. The prioritization is based on an eigenvector sensitivity analysis of a finite element model of the structure. In addition, the dual problem is presented and solved, which determines the observability of change in the measured eigenstructure from the instrumented degrees of freedom. This analysis is used to determine the extent to which damage can be localized. An analytical example is presented that illustrates the relationship between the number of measured modes, the number of instrumented degrees of freedom, and the extent to which damage can be localized. Additionally, an analysis of an experimental cantilevered eight-bay truss assembly consisting of 104 elements instrumented with eight single-axis accelerometers is presented. The extent to which structural damage can be localized from the measurement data is limited by the number of measured modes.

Introduction

FOR large space structures, practicality dictates that only partial modal data can be measured. With minimal sensor information, two questions naturally arise: At which locations should the sensors be placed, and to what extent can damage be identified with the selected sensor locations? An eigenstructure-sensitivity-based method is presented to answer these questions. Sensor placement methods have been presented by Lim,[1] Kammer,[2] and Liu and Tasker,[3] but they focused on maximizing either controllability or observability and not damage detection. Lim and Kashangaki[4] discuss which structural element failures can realistically be detected by examining modewise the percentage strain energy in each element vs the percentage measurement errors. Kashangaki[5] introduced a modal sensitivity parameter as a quantitative measure of the eigenvalue and eigenvector sensitivity, and used this to determine which modes should be used in a damage detection scheme. In practice, however, for a given complex structure, only a few of the lower-frequency global modes can be identified accurately. At higher frequencies, the separation of local and global modes becomes increasingly difficult, if not impossible. Furthermore, only a few degrees of freedom can be instrumented. Therefore, emphasis herein is placed on prioritizing sensor locations and on the ability to localize damage from partial eigendata for a given number of modes, and not on which modes to measure.

The method is based on examining the first-order partial eigenstructure sensitivity to changes in the structural stiffness of each element of a finite element model. No a priori knowledge of the damage location is assumed. Two aspects of the partial eigenstructure sensitivity are explored. First is the amount by which variations of the elemental stiffness values change the measured partial eigenstructure. Independent of the damage detection scheme used, elements that produce little or no change in the measured data will be difficult or impossible to detect when damaged. Second is the direction of change in the partial eigenstructure. Elements that produce similar or identical changes in the partial eigenstructure will be difficult or impossible to distinguish between when damaged. Therefore, sensor locations are chosen so that the change in the measured partial eigenstructure due to damage is maximized. Localization of the damage to an element(s) is based on both the amount and the direction of change to the partial eigendata for the chosen sensor locations.

Received June 10, 1996; revision received Oct. 28, 1996; accepted for publication Oct. 28, 1996; also published in *AIAA Journal on Disc*, Volume 2, Number 2. This paper is declared a work of the U.S. Government and is not subject to copyright protection in the United States.

*Captain, U.S. Air Force; currently Captain, U.S. Air Force, U.S. Air Force Phillips Laboratory, PL/VTSS, Kirtland Air Force Base, NM 87117-5776. Member AIAA.

†Associate Professor, Department of Aeronautics and Astronautics. Senior Member AIAA.

Theory

Eigenvalue and eigenvector sensitivity to changes in structural elements will be based on the finite element model of the structure. For on-orbit damage scenarios of large flexible space structures, two assumptions are made. First, structural damage is confined to changes in the stiffness properties of the structure. Second, structural damping is negligible. With these assumptions, the free vibration of the structure is modeled as

$$M\ddot{\boldsymbol{x}} + (K - \Delta K)\boldsymbol{x} = 0 \tag{1}$$

with the symmetric mass and stiffness matrices $M, K \in \Re^{n \times n}$, and $\ddot{\boldsymbol{x}}$ denoting a double time differentiation on the state vector $\boldsymbol{x}$. The matrix ΔK represents an unknown perturbation to the stiffness as the result of structural damage. The eigenvalue and eigenvector for the ith mode of Eq. (1) is given as (λ_i, Φ_i), whereas the measured eigenvalue and partial eigenvector for the same mode is represented as $(\bar{\lambda}_i, \bar{\phi}_i)$. The relationship between the n dimensional eigenvectors Φ_i and the s dimensional partial eigenvectors ϕ_i is $\phi_i = C\Phi_i$. The matrix $C \in \Re^{s \times n}$ maps the full-length eigenvector into the partial eigenvector corresponding to the measured degrees of freedom. With minimal sensor information available, a natural cost function representing the mismatch between the eigenstructure of the finite element model and the measured eigendata is

$$J = \sum_{i}^{r} a_i \left(\frac{\lambda_i}{\bar{\lambda}_i} - 1 \right)^2 + \sum_{i}^{r} \sum_{j}^{s} b_{ij} (\phi_{ij} - \bar{\phi}_{ij})^2 \tag{2}$$

Of interest for sensor location determination is how to choose the matrix C such that structural damage results in observable changes in $\bar{\lambda}_i$ and $\bar{\phi}_i$ and hence in J. Once C is determined, damage localization is concerned with the uniqueness of changes in $\bar{\lambda}_i$ and $\bar{\phi}_i$ and hence in J, for variations in the matrix ΔK in Eq. (1).

Consistent with the finite element formulation, the structural constraint can be imposed on ΔK by expressing it as

$$\Delta K = BGB^T \tag{3}$$

where B is constructed from the nodal connectivity information and the elemental parameters. For a truss structure constructed from p rod elements, B and G are written as

$$B = [B_1 \ldots B_p] \tag{4}$$

$$B_i = \sqrt{A_i E_i / L_i} \times [0, \ldots, 0, c_1, c_2, c_3, 0, \ldots, 0, -c_1, -c_2, -c_3, 0, \ldots, 0]^T \tag{5}$$

$$G = \mathrm{diag}(g_1 \ldots g_p) \qquad 0 \leq g_i \leq 1 \tag{6}$$

with c_1, c_2, c_3 representing the direction cosines for the ith element, inserted at the degrees of freedom associated with the ith element. The variables A_i, E_i, and L_i are the cross-sectional area, elastic modulus, and length of the ith element, respectively. A damage fraction value of $g_i = 0$ corresponds to an undamaged element, whereas $g_i = 1$ corresponds to a complete loss of stiffness to the ith element. A further discussion on constructing the BGB^T parameterization can be found elsewhere.[6]

The eigenvalue and eigenvector sensitivity to structural damage is computed on the basis of the method presented by Fox and Kapoor.[7] However, with damage confined to the stiffness matrix, the calculations are further simplified. The eigenvalue equation is written as

$$(-\lambda_i M + K - BGB^T)\Phi_i = 0 \tag{7}$$

With the assumption that changes from structural damage are confined to the perturbation matrix ΔK and hence the vector $\boldsymbol{g}$, Eq. (7) is differentiated, which after simplifying results in

$$M\Phi_i \frac{\partial \lambda_i}{\partial \boldsymbol{g}} + \frac{\partial}{\partial \boldsymbol{g}}(BGB^T\Phi_i) = 0 \tag{8}$$

To simplify the partial derivative term in Eq. (8), the matrix operator $P(\alpha, \beta)$ is introduced and defined as

$$P(\alpha, \beta) \quad \text{with} \quad P, \beta \in \Re^{n\times p}, \qquad \alpha \in \Re^{n\times 1}$$
$$P_{ij} = \sum_{k=1}^{n} \alpha_k \beta_{ij} \beta_{kj} \tag{9}$$

where P_{ij} is the ith row and the jth column of the matrix P. In terms of the operator P, the matrix product in parenthesis in Eq. (8) can be written as

$$BGB^T\Phi_i = P(\Phi_i, B)\boldsymbol{g} \quad \text{where} \quad \boldsymbol{g} = \mathrm{diag}(G)$$
$$G \in \Re^{p\times p}(\mathrm{diag}) \tag{10}$$

Each eigenvector is normalized so that $\Phi_i^T M\Phi_i = 1$. Premultiplying Eq. (8) by Φ_i^T and using the operator P, the eigenvalue sensitivity from Eq. (8) can be written as

$$\frac{\partial \lambda_i}{\partial \boldsymbol{g}} = -\Phi_i^T P(\Phi_i, B), \qquad \frac{\partial \lambda_i}{\partial \boldsymbol{g}} \in \Re^{1\times p} \tag{11}$$

In a similar fashion, eigenvector sensitivity is computed by differentiating Eq. (7) and using the results of Eq. (11). The eigenvector sensitivity for the ith mode is

$$[K - \lambda_i M - BGB^T]\frac{\partial \Phi_i}{\partial \boldsymbol{g}} = [M\Phi_i\Phi_i^T + I]P(\Phi_i, B)$$
$$\frac{\partial \Phi_i}{\partial \boldsymbol{g}} \in \Re^{n\times p} \tag{12}$$

The matrix I denotes the $n \times n$ identity matrix. The method introduced by Nelson[8] is used to solve Eq. (12). This is necessary because of the singularity of the matrix $[K - \lambda_i M - BGB^T]$. Assuming no repeated roots, this method involves separating the solution into a particular and homogeneous solution, where

$$\frac{\partial \Phi_i}{\partial \boldsymbol{g}} = \Phi_i c_i + V_i \tag{13}$$

with

$$\tilde{V}_i = [\tilde{K} - \lambda_i \tilde{M} - \tilde{B}\tilde{G}\tilde{B}^T]^{-1}[\tilde{M}\tilde{\Phi}_i\tilde{\Phi}_i^T + \tilde{I}]\tilde{P}(\Phi_i, B) \tag{14}$$

and

$$V_i = [\tilde{V}_{i1}, \ldots, \tilde{V}_{il-1}, 0, \tilde{V}_{il}, \ldots, \tilde{V}_{in-1}]^T \tag{15}$$

The $(\tilde{\ })$ notation represents matrices reduced by one row and one column, or vectors reduced by one element. Nelson's method removes the row and column corresponding to the maximum entry in Φ_i. Equation (15) corresponds to the maximum entry occurring at the lth element. For computational efficiency, a decomposition and substitution is preferable to explicitly computing the inverse. The constant row vector $\boldsymbol{c}_i$ is given as

$$\boldsymbol{c}_i = -\Phi_i^T M V_i \tag{16}$$

With the first-order eigenvalue and eigenvector sensitivities defined, let $\nabla\lambda$ be the matrix whose ith row and jth column entry is defined as

$$\nabla\lambda_{ij} = \frac{\partial \lambda_i}{\partial \boldsymbol{g}_j} \cdot \frac{1}{\lambda_i} = -\frac{\Phi_i^T P(\Phi_i, B_j)}{\lambda_i} \tag{17}$$

The term λ_i is introduced to correct the scaling of the different modes. With this definition, each column of the matrix $\nabla\lambda$ corresponds to different structural elements and each row of the matrix to a different mode. The change in eigenvalue due to changes in the structural elements $\Delta\boldsymbol{g} \in \Re^{p\times 1}$, to first order, is given as

$$\Delta\lambda = \nabla\lambda\Delta\boldsymbol{g} \tag{18}$$

where

$$\Delta\lambda = [\Delta\lambda_1, \ldots, \Delta\lambda_r]^T \quad \text{and} \quad \Delta\lambda_i = \frac{\lambda_i - \lambda_{oi}}{\lambda_{oi}}$$
$$\forall i = 1, \ldots, r \tag{19}$$

The vector $\Delta\lambda \in \Re^{r\times 1}$ consists of the fractional changes in the r measured eigenvalues of the structure due to damage. Similarly, the vector $\Delta\lambda_o \in \Re^{r\times 1}$ contains the eigenvalues of the structure evaluated at BG_oB^T. For the undamaged structure, $BG_oB^T = 0$. Because Eq. (18) is valid only for small changes of $\Delta\boldsymbol{g}$, it is not possible to use it directly to determine damaged elements. However, for the purpose used herein, Eq. (18) is adequate to examine the relationship between $\Delta\lambda$ and $\Delta\boldsymbol{g}$. Information on the amount and direction of changes in $\Delta\lambda$ are contained in the matrix $\nabla\lambda$. With $0 < g_i < 1$, rows of $\nabla\lambda$ with very small norms will contribute negligibly to changes in $\Delta\lambda$. Rows in $\nabla\lambda$ that are similar or identical to one another will have values of $\Delta\boldsymbol{g}_i$ that affect $\Delta\lambda$ similarly or identically, and hence will be indistinguishable from one another. For this analysis, it is assumed that $\|\boldsymbol{g}\|_2$ is small and that, although individual elements in $\Delta\boldsymbol{g}$ may be close to unity, the overall effect on the global nature of the structure is small, i.e., no catastrophic failures.

Using the results from Eq. (12), the partial eigenvector sensitivity for the ith mode is defined as

$$\nabla\phi_i = C\frac{\partial \Phi_i}{\partial \boldsymbol{g}}, \qquad \nabla\phi_i \in \Re^{s\times p} \tag{20}$$

where C is determined from the measured degrees of freedom as previously defined. With this definition, changes in the partial eigenvector for the ith mode, to first order in $\Delta\boldsymbol{g}$, is given as

$$\Delta\phi_i = \nabla\phi_i\Delta\boldsymbol{g} \quad \text{where} \quad \Delta\phi_i = \phi_i - \phi_{i_o} \tag{21}$$

The vector $\phi_i \in \Re^{s\times 1}$ is the partial eigenvector for the instrumented degrees of freedom, and $\phi_{i_o} \in \Re^{s\times 1}$ contains the partial eigenvector of the finite element model evaluated at BG_oB^T. Similar to the eigenvalue case, information on the amount and direction of change of $\Delta\phi_i$ is contained in the matrix $\nabla\phi_i$. Note that there is one matrix $\nabla\phi_i$ for each measured mode. Information on which to base both sensor location and damage localization is contained in the matrices $\nabla\lambda$ and $\nabla\phi_i$. Two properties of these matrices are investigated, which are referred to as the detectability and colinearity. Detectability is a measure of the amount of change that occurs from changes in a design variable, whereas colinearity is a measure of the direction of change.

Sensor Location Prioritization

Initially with $C = I$ (the identitiy matrix), $\nabla\phi_i$ from Eq. (20) contains information indicating which degrees of freedom to instrument. As previously discussed, in a typical flexible structure only a few of the low-frequency modes can be measured. Given this fact and the problem of solution nonuniqueness associated with using partial measurement data, it is assumed that any mode that can be measured should be used in a damage detection scheme. Given then that there are r measured modes, the detectability in the measured eigenvectors at the lth degree of freedom from changes in the p elements of the structure is defined as

$$D_{\phi_l} = \sum_{k=1}^{p}\sum_{i=1}^{r}\left|[\nabla\phi_i]_{lk}\right| \tag{22}$$

The vector $\boldsymbol{D}_\phi = [D_{\phi_1} \ldots D_{\phi_n}]^T$ is then sorted in descending order, initially prioritizing the sensor locations on the basis of detectability. A threshold is set on the basis of measurement uncertainty and the finite element modeling errors. Values of D_{ϕ_l} below this threshold indicate degrees of freedom that are unaffected by structural damage for the measured modes. Next, a colinearity check is made to determine degrees of freedom that yield similar information on the damaged elements. The colinearity, denoted S, between any two vectors α and β is defined as

$$S_{\alpha\beta} = \alpha^T\beta \qquad \|\alpha\|_2 = \|\beta\|_2 = 1 \tag{23}$$

A value of $S_{\alpha\beta} = 1$ indicates perfect colinearity, whereas $S_{\alpha\beta} = 0$ indicates orthogonal vectors. With this definition, the colinearity of the eigenvector sensitivity between measured degrees of freedom l and m is defined as

$$S_{\phi_{lm}} = \left[\frac{1}{r}\sum_{i=1}^{r}[\nabla\phi_i \cdot \nabla\phi_i^T]\right]_{lm} \tag{24}$$

Again, a threshold from unity is set on the basis of measurement uncertainty and the finite element modeling errors. Values in $S_\phi \in \Re^{n\times n}$ within this threshold are declared colinear, indicating that at these degrees of freedom for the r measured modes, the changes in the eigenvector are indistinguishable from one another to changes in the structural elements. Using this information, multiple colinear entries in vector $\boldsymbol{D}_\phi$ are removed, leaving only one entry from each colinear grouping. The remaining first s elements of vector $\boldsymbol{D}_\phi$ represent the prioritized s degrees of freedom to place sensors. With $\boldsymbol{D}_\phi^s$ defined as the first s elements of the reduced and sorted vector $\boldsymbol{D}_\phi$, the matrix C is chosen such that $\boldsymbol{D}_\phi^s = C\boldsymbol{D}_\phi$ is satisfied. An analytical example is presented in a subsequent section, following the discussion of damage localization.

Damage Localization

Given the r modes measured at the s degrees of freedom as determined above, damage localization determines the extent to which damage can be isolated to individual elements. Similar detectability and colinearity metrics are used, which now are restricted to the instrumented degrees of freedom. The detectability in the measured eigenvalues from changes in the kth structural element is defined as

$$D_{\lambda_k} = \sum_{i=1}^{r}\left|\nabla\lambda_{ik}\right| \tag{25}$$

where $\boldsymbol{D}_\lambda = [D_{\lambda_1} \ldots D_{\lambda_p}]^T$. Eigenvalue colinearity information is contained in S_λ. The jth row and kth column of S_λ indicates the colinearity of the eigenvalue changes between the jth and kth structural elements and is defined as

$$S_{\lambda_{jk}} = [\nabla\lambda^T \cdot \nabla\lambda]_{jk} \tag{26}$$

Note that the eigenvalue colinearity is independent of the degree of freedom at which it is measured. Similarly, detectability in the measured eigenvectors from the kth structural element is defined as

$$D_{\phi_k} = \sum_{l=1}^{s}\sum_{i=1}^{r}\left|[\nabla\phi_i]_{lk}\right| \tag{27}$$

where $\boldsymbol{D}_\phi = [D_{\phi_1} \ldots D_{\phi_p}]^T$. Eigenvector colinearity information is contained in S_ϕ. The jth row and kth column of S_ϕ indicates the colinearity of the eigenvector changes between the jth and kth structural elements and is defined as

$$S_{\phi_{jk}} = \left[\frac{1}{r}\sum_{i=1}^{r}[\nabla\phi_i^T \cdot \nabla\phi_i]\right]_{jk} \tag{28}$$

Note the similarity between Eqs. (22) and (24) and Eqs. (27) and (28). For this reason, sensor prioritization and damage localization are considered dual problems, either of which can be determined with only a slight modification to the same algorithm. Notationally, detectability $\boldsymbol{D}$ and colinearity S were multiply defined, once for sensor prioritization and again for damage detection. It should be clear from the context of the problem which definition applies.

With these definitions, damage localization proceeds as follows. Elements in $\boldsymbol{D}_\lambda$ and $\boldsymbol{D}_\phi$ that are below the modeling and measurement uncertainty threshold level are declared undetectable. Thus, because of modeling and measurement uncertainties, damage in an undetectable element cannot be identified from the measured data. Of the remaining (i.e., detectable) elements, colinear elements as indicated by elements in S_λ and S_ϕ above the uncertainty level are indistinguishable from one another. Thus, from the measured data, structural damage can be localized only to a colinear group, and not to an individual element within the group. Elements contained in a colinear group are referred to as symmetric elements.

Software Implementation

The sensor prioritization and damage localization method was implemented using MATLAB® [Ref. 9] software. For a given number of modes, the eigenvalue and eigenvector sensitivities are computed using Eqs. (11) and (13), respectively. From these, the detectability metrics $\boldsymbol{D}_\lambda$ and $\boldsymbol{D}_\phi$ are computed using Eqs. (25) and (27). The colinearity metrics S_λ and S_ϕ are computed using either Eqs. (22) and (24) for sensor prioritization or using the transposes as given in Eqs. (26) and (28) for damage localization. These metrics then are compared against threshold values based on assumed model and measurement uncertainty. The uncertainty is determined by how well the finite element model correlates with the measured data, for nominal as well as damage configurations. The detectability threshold was established as a percentage of the maximum element in the vector $\boldsymbol{D}$. For colinearity the threshold was a percentage decrease from unity value. With the thresholds established, the elements of the structure then are classified as either undetectable (U) using $\boldsymbol{D}_\lambda$ and $\boldsymbol{D}_\phi$, or symmetric (S), or identifiable (I) using S_λ and S_ϕ. For computational efficiency, detectability is checked first. All elements with values below the detectability threshold are classified as U and are removed from the sensitivity gradient matrices before forming the colinearity metrics. Colinearity groupings then are determined from the colinearity matrix by replacing the entries of the matrix with either ones or zeros based on being above or below the colinearity threshold. In this way, a nonzero entry in the ith row and jth column indicates symmetry between the ith and jth elements. Note that only the entries above the main diagonal need to be computed. Based on these entries, the elements are classified as either S or I. For a colinear grouping of elements as determined by S_λ and S_ϕ, one element in the group is classified as I and the remaining elements in the group as S. The selection of the weighting between emphasis on S_λ and on S_ϕ is dependent on the damage identification scheme used. For damage identification based on the cost function minimization, given in Eq. (2), the metric results should be combined consistently with the cost-function weighting coefficients. For example, a high relative weighting on the eigenvalues corresponds to an increased emphasis on the $\boldsymbol{D}_\lambda$ and S_λ metrics. A decision flow chart for the damage localization process as implemented for use with an assigned partial eigenstructure (APE) approach as presented

Table 1 Damage localization results for a 41-element free–free planar truss

No. of sensors	Measured flexible modes: 1	1, 2	1, 2, 3	1, 2, 3, 4	1, 2, 3, 4, 5
1	29/9/3[a]	21/15/5	21/15/5	9/25/7	9/24/8
2	29/9/3	21/8/12	21/3/17	9/6/26	9/1/31
3	29/2/10	21/2/18	21/0/20	9/3/29	9/1/31
4	29/0/12	21/1/19	21/0/20	9/4/28	9/0/32
5	29/0/12	21/3/17	21/0/20	9/3/29	9/0/32
6	29/0/12	21/3/17	21/0/20	9/2/30	9/0/32
Locations[b]	34, 2, 1, 3, 33, 35	1, 35, 3, 33, 9, 27	1, 35, 33, 3, 36, 2	1, 35, 33, 3, 36, 2	1, 35, 3, 33, 16, 22

[a] Data presented in U/S/I format where U denotes the number of undetectable elements, S the number of symmetric elements, and I the number of identifiable elements. The sum of U, S, and I equals the total number of elements of the structure.
[b] The locations of the sensors were chosen by use of the prioritization method presented and are reported by degree of freedom number in prioritized order.

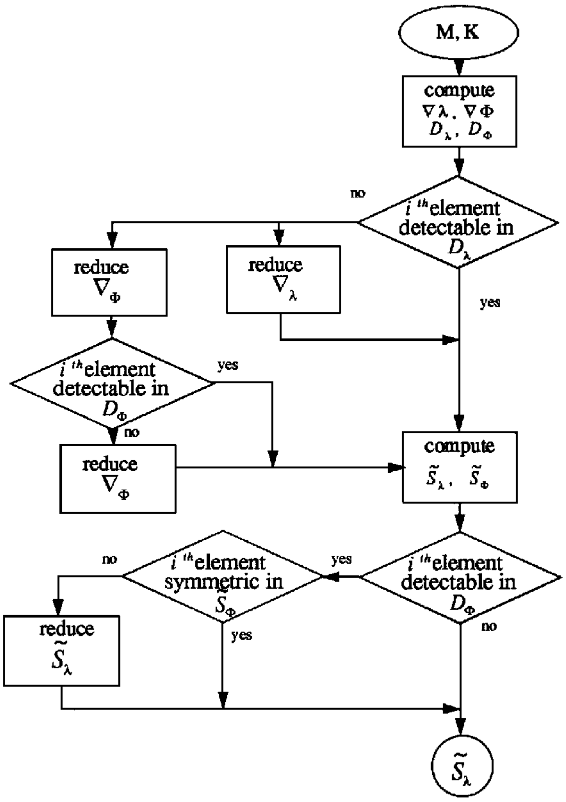

Fig. 1 Damage localization decision flow.

by Cobb and Liebst[6] is shown in Fig. 1. The decision chart reflects the emphasis that the APE method places on eigenvalues over the eigenvectors. The U/S/I classification is determined directly from the resulting $\tilde{S}_\lambda$ matrix. Rows and columns removed from S_λ to form $\tilde{S}_\lambda$ correspond to U elements. Entries in $\tilde{S}_\lambda$ with a unity value indicate symmetry between the elements corresponding to the row and column position.

Independent of the algorithm used for damage identification, the advantage of the U/S/I classification is apparent. It quickly indicates which damaged elements cannot be detected from the measured data. Furthermore, only elements in the I classification need to be included in the search space of possible failed elements, typically resulting in much improved algorithm convergence speed.[6]

Analytical Example

To demonstrate the use of the detectability and colinearity metrics, an analytical example of both the sensor prioritization and damage localization was performed using a 41-element free–free planar truss assembly as shown in Fig. 2. The truss was modeled using 41 rod elements, with two translational degrees of freedom per node. All members are aluminum of 1-in.^{2} cross section, with the vertical and horizontal members 30 in. long.

The first analysis was an examination of the relationship between increasing the number of measured modes and increasing the number of sensors. The results are presented in Table 1. The data clearly show that, if possible, increasing the number of modes measured is preferable to increasing the number of sensors to enhance damage localization. For all cases, the threshold values were fixed at 10% for detectability and 5% colinearity, meaning values in $\boldsymbol{D}_\lambda$ and $\boldsymbol{D}_\phi$ of less than 10% of the maximum values in these metrics were declared undetectable. Similarly, values of the inner products in S_λ and S_ϕ of greater than 95% were declared colinear. Note that the tabulated results in some instances show that adding additional sensors had an adverse effect on identifiability. This trend is an artifact of using different-length vectors, due to a different number of sensors, compared against a fixed threshold. The data as presented are intended only to show the overall trends.

To demonstrate sensor prioritization, the locations of three sensors were selected by use of a fixed number of modes and the same thresholds as stated above. As shown in Table 2, the prioritized locations increase the number of identifiable elements over two randomly chosen sensor locations.

Table 2 Damage localization for different sensor locations for a 41-element free–free planar truss

Method	Sensor location[a]	Damage localization (U/S/I)[b]
Prioritized	1, 35, 3	9/1/31
Random	3, 11, 19	9/5/27
Random	2, 4, 34	9/3/29

[a] Reported by degree of freedom number.
[b] Based on measuring the first five flexible modes, using three sensors.

Table 3 Damage localization based on eigenvalue sensitivity using the first five flexible modes, for the 41-element free–free planar truss

Element no.	Equivalent symmetric elements, S_λ [a]
2	5, 37, 40
3	4, 38, 39
7	10, 32, 35
8	9, 33, 34
12	15, 27, 30
13	14, 28, 29
17	20, 22, 25
18	19, 23, 24
Undetectable elements	1, 6, 11, 16, 21, 26, 31, 36, 41

[a] Results are independent of selected sensor location.

A third analysis was performed to demonstrate the validity of using only first-order sensitivities, evaluated at the nominal configuration, over the range of $\Delta\boldsymbol{g}$. Table 3 lists the symmetric elements as determined by S_λ for the first five flexible modes, for the same threshold values as used above and using a single sensor. As an example, the results indicate that elements 8, 9, 33, and 34 are symmetric to the partial measured data, and thus only one element should be included in the damage-detection search space. The measured eigenvalues with damage to element 8 corresponds

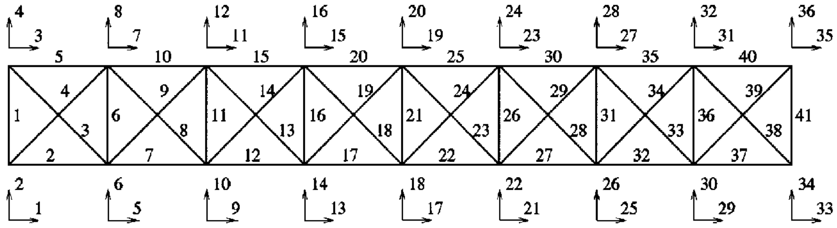

Fig. 2 A 41-element free–free truss showing degree of freedom and element numbering.

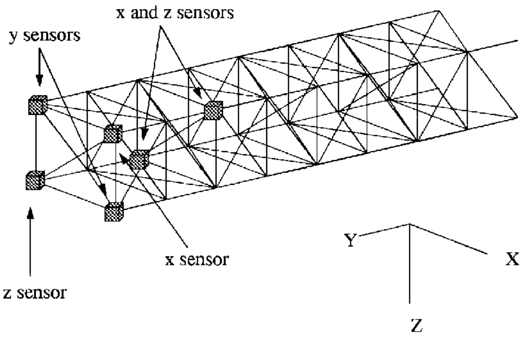

Fig. 3 Prioritized sensor locations for the NASA truss.

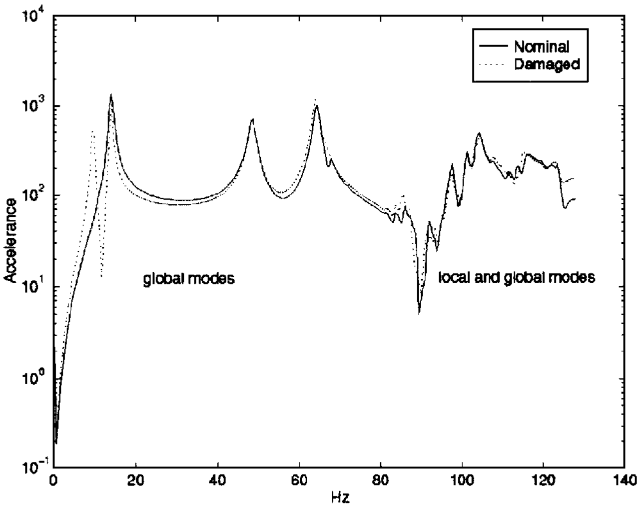

Fig. 4 Measured frequency response functions for the NASA truss.

to the same eigenvalues for an equivalent break in either elements 9, 33, or 34. For an example with multiple breaks, elements 8 and 30 were reduced by 70 and 50%, respectively. Using any combination of two elements, selecting one element from the symmetric set (8, 9, 33, 34), and one element from the symmetric set (12, 15, 27, 30), reduced by 70 and 50% respectively, the changes in the measured eigenvalues were within 2% of each other. This is well within the uncertainty level established in the threshold for S_λ used to select the symmetric sets.

Experimental Demonstration

An experimental validation of the sensor prioritization and damage localization method was conducted using NASA test data of an experimental truss. NASA's eight-bay truss test bed consisted of eight cubic bays of a hybrid space truss cantilevered from a rigid backstop plate (see Fig. 3). This configuration represents a scaled section of the proposed International Space Station. Each bay is a half meter long and constructed of aluminum members. The truss was fully instrumented with one triaxial accelerometer at each of its 32 unconstrained nodes. Disturbance excitation was achieved using two ground-based dynamic shakers attached at two different node points. Figure 4 shows a typical measured frequency response function for both the nominal and the damaged structure. From these frequency responses, the first five system natural frequencies could be determined. A complete description of the hardware and the testing procedure is contained in the work by Kashangaki.[10]

Table 4 Damage localization results for the NASA eight-bay truss

Element no.	Equivalent symmetric elements
32	36, 45, 49
34	38
47	51, 60, 64
58	62, 71, 75
59	
61	
63	
65	
72	
73	77, 86, 90
74	
76	
78	
84	88, 97, 101
85	
87	
89	
91	
98	
99	103
100	
102	
104	
Undetectable elements	1–31, 33, 35, 37, 39–44, 46, 48, 50, 52–57, 66–70, 79–83, 92–96

After tuning the analytical model using the method described by Cobb et al.,[11] a prioritization of which degrees of freedom to instrument was performed as developed previously. To demonstrate the use of limited sensor measurements, a small number of sensors (8) were chosen. Threshold values of 10% for detectability and 7% for colinearity were used for both the sensor prioritization and the damage localization method. These threshold values represent the assumed combined uncertainty in both the measurement error and the modeling error. These values were chosen by performing three analyses for threshold values of 5, 7, and 10%, and then comparing overall results against measured and analytical simulations of structural damage. The eight prioritized sensor locations are shown in Fig. 3. These eight degree-of-freedom locations were used to construct the eight elements of the partial eigenvectors for the damage identification process.

Having identified the sensor locations, a damage localization analysis was performed. The results of this analysis are contained in Table 4, listing the undetectable, symmetric, and identifiable elements. Table 5 presents a description of the element numbering used. The results show that using only the first 5 modes and the 8 component eigenvectors, 64 of the elements are undetectable from the measured data. This indicates that changes in the measured data are insignificant from damage in these elements. These results are consistent with a similar analysis on this truss presented by Kashangaki, et al.,[12] showing that 95% of the total strain energy associated with the first six modes was contained in only 40 elements. The unidentifiable elements are categorized as either battens or elements located near the free end of the truss. The remaining 40 elements of the localization analysis are divided among 23 symmetric groupings containing 1, 2, or 4 elements. One element from each of the 23 symmetric groups is used to define the initial search space for the identification process.

Nine damage cases were tested. The damage cases were the full removal of one or two elements of the truss. Using the results of the sensor prioritization to define the measured data, the tuned

Table 5 Element numbering and descriptions for the NASA eight-bay truss

	Description		
Bay no.[a]	Longeron	Diagonal	Batten[b]
1	6, 8, 10, 12	7, 9, 11, 13	1, 2, 3, 4, 5
2	19, 21, 23, 25	20, 22, 24, 26	14, 15, 16, 17, 18
3	32, 34, 36, 38	33, 35, 37, 39	27, 28, 29, 30, 31
4	45, 47, 49, 51	46, 48, 50, 52	40, 41, 42, 43, 44
5	58, 60, 62, 64	59, 61, 63, 65	53, 54, 55, 56, 57
6	71, 73, 75, 77	72, 74, 76, 78	66, 67, 68, 69, 70
7	84, 86, 88, 90	85, 87, 89, 91	79, 80, 81, 82, 83
8	97, 99, 101, 103	98, 100, 102, 104	92, 93, 94, 95, 96

[a]Bays are numbered consecutively starting from the free end.
[b]Includes diagonal members in the batten plane.

Table 6 APE identification results on the NASA truss, sparsely instrumented

	True damage		APE identified		
Damage case	Element no.	Damage, %	Element no.	Damage, %	CPU time, s
A	84	100	84(88, 97, 101)[a]	85	33
B	85	100	85	96	80
C	71	100	58(62, 71, 75)	94	65
D	78	100	78	98	76
			104	110	
E	62	100	58(62, 71, 75)	110	56
			32(36, 45, 49)	103	
F	97	100	84(88, 97, 101)	89	32
G	51	100	47(51, 60, 64)	88	85
H	34	100	34(38)	97	43
I	71	100	32(36, 45, 49)	80	63
	78	100	78	99	

[a]Data presented in I(S) format, where I is the number of the identified element and S is the symmetric element numbers.

analytical model, and the damage localization analysis to define the initial search space, damage identification using APE as described previously[6] was performed. The results are contained in Table 6. In six of the nine cases, the damage was localized to a single element or a single symmetric grouping. For cases D and E, a repeated use of the APE method, using the results of the first identification application as the initial search space, was able to localize the damage down to the single correct element or single symmetric group. For damage case I, the compound break, damage to element no. 71 was not identified. Damage to element no. 71 (a longeron in the sixth bay) was assigned to a longeron in either bay three or bay four. This difficulty is due in part to the fact that the measured data for this damage case do not correlate well with the simulated damaged analytical model. The true culprit, modeling error or measurement error, cannot be determined from the known information. Anytime the simulated damage to the analytical model does not agree with the measured data for the same damage configuration, any method based on matching the partial measured data will have difficulty in obtaining the true solution. Without the preprocessing described herein to reduce the search space of damaged elements, the APE method[6] took on the order of 300 CPU seconds to converge. Comparing this with the CPU times in Table 6, we see that determining undetectable and symmetric elements before damage identification results in significant improvements.

Conclusions

A method is presented that prioritizes the degrees of freedom to instrument when used to collect modal data for damage identification. It was shown that this method also can be used to determine the extent to which damage can be localized from these sensor locations. The method represents a computationally attractive alternative to an exhaustive search over the parameter space and is a valuable tool during the design phase to determine measurement and/or modeling accuracy requirements. An analytical example is presented that shows that the extent to which damage can be localized is limited by the amount and quality of the measured data. It is also shown that increasing the number of measured modes is of greater benefit than increasing the number of sensors. The method was applied to a sparsely instrumented experimental truss. The results show that the extent to which damage can be localized is limited by the amount of modal information available. However, in each case, damage could be localized to a small section of the structure. CPU times for damage identification are shown to be significantly improved by using the damage localization method presented.

Acknowledgment

Special thanks to T. Kashangaki, who provided the experimental data on the NASA truss.

References

[1]Lim, K. B., "A Method for Optimal Actuator and Sensor Placement for Large Flexible Space Structures," *Proceedings of the AIAA Guidance, Navigation, and Control Conference*, AIAA, Washington, DC, 1990, pp. 1352–1356.

[2]Kammer, D. C., "Sensor Placement for On-Orbit Modal Identification and Correlation of Large Space Structures," *Journal of Guidance, Control, and Dynamics*, Vol. 14, No. 9, 1991, pp. 251–259.

[3]Liu, C., and Tasker, F. A., "Sensor Placement for Multi-Input Multi-Output Dynamic Identification," *Proceedings of the 36th Structures, Structural Dynamics, and Materials Conference*, AIAA, Washington, DC, 1995, pp. 3327–3337.

[4]Lim, T. W., and Kashangaki, T. A., "Structural Damage Detection of Space Truss Structures Using Best Achievable Eigenvectors," *AIAA Journal*, Vol. 32, No. 5, 1994, pp. 1049–1057.

[5]Kashangaki, T. A. L., "Mode Selection for Damage Detection Using the Modal Sensitivity Parameter," *Proceedings of the 33rd Structures, Structural Dynamics, and Materials Conference*, AIAA, Washington, DC, 1992, pp. 1535–1542.

[6]Cobb, R. G., and Liebst, B. S., "Structural Damage Identification Using Minimal Sensor Information," *Proceedings of Identification in Engineering Systems*, Univ. of Wales, Swansea, Wales, UK, 1996, pp. 285–294.

[7]Fox, R. L., and Kapoor, M. P., "Rates of Change of Eigenvalues and Eigenvectors," *AIAA Journal*, Vol. 6, No. 12, 1968, pp. 2426–2429.

[8]Nelson, R. B., "Simplified Calculation of Eigenvector Derivatives," *AIAA Journal*, Vol. 14, No. 9, 1976, pp. 1201–1205.

[9]Anon., "Matlab®: High Performance Numeric Computation and Visualization Software," MathWorks, Inc., Natick, MA, 1994.

[10]Kashangaki, T. A. L., "Ground Vibration Tests of a High Fidelity Truss for Verification of On Orbit Damage Location Techniques," NASA TM-107626, May 1992.

[11]Cobb, R. G., Canfield, R. A., and Liebst, B. S., "Finite Element Model Tuning Using Automated Structural Optimization System Software," *AIAA Journal*, Vol. 34, No. 2, 1996, pp. 392–399.

[12]Kashangaki, T. A., Smith, S. W., and Lim, T. W., "Underlying Modal Data Issues for Detecting Damage in Truss Structures," *Proceedings of the 33rd Structures, Structural Dynamics, and Materials Conference*, AIAA, Washington, DC, 1992, pp. 1437–1446.